Available online at www.sciencedirect.com

ScienceDirect

Ceramics International 34 (2008) 63–68

CERAMICS INTERNATIONAL

www.elsevier.com/locate/ceramint

Influence of magnesia on the structure and properties of $MgO-Al_2O_3-SiO_2-F^-$ glass-ceramics

Liping Yu [a,b], Hanning Xiao [a,*], Yin Cheng [a]

[a] College of Materials Science and Engineering, Hunan University, Changsha, Hunan 410082, PR China
[b] College of Chemistry and Chemical Engineering, Hunan Normal University, Changsha, Hunan 410081, PR China

Received 17 May 2006; received in revised form 3 July 2006; accepted 22 August 2006
Available online 7 February 2007

Abstract

Effects of MgO content (13.4–31.4 mol%) on the structure and properties of $MgO-Al_2O_3-SiO_2-F^-$ glass-ceramics were investigated by differential scanning calorimetry (DSC), X-ray diffractometry (XRD), infrared spectrophotometry (IR) and scanning electron microscopy (SEM). Results show that the main units of glass network structure are [SiO_4] and [AlO_4]. MgO contributes to the weakening of silica network and reduce the stability of glass structure. The main crystals of the $MgO-Al_2O_3-SiO_2-F^-$ glass-ceramics are phlogopite, spinel, flur-pargrasite and forsterite. The increase of reheating temperature and MgO content are beneficial to the separation of phlogopite crystal, and cause an higher aspect ratio of the phlogopite phase, which improves the machinability of the glass-ceramics. Excellent machinability is obtained when MgO content is 31.4 mol% at the processing temperature of 1100 °C for 2 h.

Keywords: $MgO-Al_2O_3-SiO_2-F^-$ glass-ceramics; Machinablity; Mica; Microstructure; Crystallization

1. Introduction

Glass-ceramics are a kind of polycrystalline materials by controlled crystallization from glasses [1]. Mica-containing glass-ceramics, in particular of the phlogopite system, are of technical interest due to their machinability. In 1970, Beal et al. [2] reported machinable glass-ceramics containing phlogopite from the $SiO_2-B_2O_3-MgO-Al_2O_3-K_2O-F^-$ glass system. Grossman [3] obtained tetrasilicic-mica glass-ceramics from the $K_2O-MgF_2-MgO-SiO_2$ glass system. The structure of phlogopite is composed of a two-dimensional network of corner-shared [SiO_4]- and [AlO_4]-tetrahedra, forming an hexagonal ring. A layer of Mg^{2+} ions in octahedral coordination is located between two tetrahedral layers. The triple layers are connected to each other by relatively large alkali ions, e.g., K^+ or Na^+. Because of weak bonding of alkali layer, crack propagation takes place preferentially along the (0 0 1) cleavage plane [4].

Shape and volume of mica crystals have an important influence on machinability of glass-ceramics. Cabbage-shaped mica crystal aggregates can be obtained from special glass compositions and bending radii of mica aggregates are sensitively dependent on heating rates [5]. The machinability of glass-ceramics containing cabbage-shaped mica is four or five times than that of glass-ceramics containing mica plate [6]. By using hot-pressing technique, the bending strength and fracture toughness of oriented materials can be improved up to 380 and 2.8 MPa $m^{1/2}$, respectively [7,8]. Crystal alignment reduced the machinability by about 50% [9].

Few systematic studies may be found on the influence of glass compositions on the formation of fluorphlogopite crystal phase. Henry reports that addition of Li_2O can decrease the glass transition temperature [10] and increase the aspect ratio of the mica crystals [11]. Addition of PbO and P_2O_5 to the basic glass also changed the mica crystals morphology from platelet to spherical shapes [12].

Mg^{2+} is an important component of the mica structure, so MgO content affect the glass structure and the formation or shape of mica crystals. This study aims at investigating the influence of MgO on the structure and properties of $MgO-Al_2O_3-SiO_2-F^-$ glass-ceramics.

---

* Corresponding author. Tel.: +86 731 8822269.
E-mail address: hnxiao@hnu.cn (H. Xiao).

0272-8842/$32.00 © 2006 Elsevier Ltd and Techna Group S.r.l. All rights reserved.
doi:10.1016/j.ceramint.2006.08.004

Table 1
Compositions of various glass samples (mol%)

Sample	SiO_2	Al_2O_3	CaO	MgO	B_2O_3	K_2O	F^-
1#	49.5	6.9	5.8	13.4	6.2	1.1	17.1
2#	43.0	6.7	5.6	20.9	6.1	1.1	16.6
3#	39.8	6.6	5.6	24.5	6.0	1.1	16.4
4#	36.7	6.6	5.5	28.0	5.9	1.1	16.2
5#	33.8	6.5	5.4	31.4	5.8	1.1	16.0

2. Experimental

Glass batches of compositions listed in Table 1 were obtained by melting Al_2O_3, $CaCO_3$, $MgCO_3$, H_3BO_3, K_2CO_3, SiO_2 and MgF_2 reagents in an alumina crucible at 1500–1600 °C for 2 h. The melts were cast into graphite molds to form 80 mm × 80 mm × 6 mm glass blocks, then cooled at a rate of 1 °C min^{-1} from 600 °C to room temperature in order to release thermal stresses. The glass blocks were subsequently reheated under special processing schedules so as to get the glass-ceramics.

Differential thermal analysis (DSC) was carried out on fine glass powders using a Netzsch STA-449C thermal analyzer with a heating rate of 10 °C min^{-1} in the temperature range from 10 to 1200 °C under air-atmosphere. Infrared absorption spectra of all samples were measured with WQF-200 spectrophotometer using the KBr pellets technique. Crystalline phases were analyzed by a Rigaku D/max 2550VB + 18 kW diffractometer. Microstructure of the specimens was observed with a JSM-5600 LV scanning electron microscope. The machinability was evaluated by the drilling depth of the glass-ceramics within 30 s, using a 6 mm hard alloy bit IDSZU-1 in a drill press of 50 kN at 500 rpm.

3. Results and discussion

Fig. 1 shows the FT-IR spectra of the glasses with magnesia content from 13.4 to 31.4 mol%. Tables 2 and 3 summarize the major observed absorption bands in the investigated glasses and their vibration types respectively. Ca^{2+}, Mg^{2+} and K^{2+} ions act as network modifiers, inducing non-bridging oxygens (NBOs), and lie in interspaces of the glass network. Al^{3+}, as a network former in peralkaline compositions[1], can substitute Si^{4+} to form $[AlO_4]$ tetrahedron [19,20]. As the molar ratio of $Al_2O_3/(CaO + MgO + K_2O)$ is less than 0.5, $[AlO_4]$ tetrahedron is easy to form in the investigated glasses. The band near 710 cm^{-1} may be specified as the stretching vibration of Al–O bond in $[AlO_4]$ tetrahedron [21]. The absorption band of the stretching vibration of $[SiO_4]$ tetrahedra lies in the range of 800–1200 cm^{-1}, while varies with the concentration of NBOs [19]. The band near 970 cm^{-1} may be attributed to a stretching vibration of the Si–O bond, in the $Si(OAl/Ca)_2$, $Si(OAl/Mg)_2$ or $Si(OAl/K)_2$ group, i.e., $[SiO_4]$ tetrahedron with two corners shared with Al–O, Ca–O, Mg–O or K–O polyhedra. Stoch and Środa [22] reports that introduction of the modifier ions (Na^+, Ca^{2+}, Mg^{2+}) causes a shift towards smaller wavenumber in the Si–O–Si stretching band, resulting from the depolymerization of the silicate framework. Therefore, it is reasonable to suggestion that MgO contributes to the weakening of silica network and reduces the stability of the glass structure.

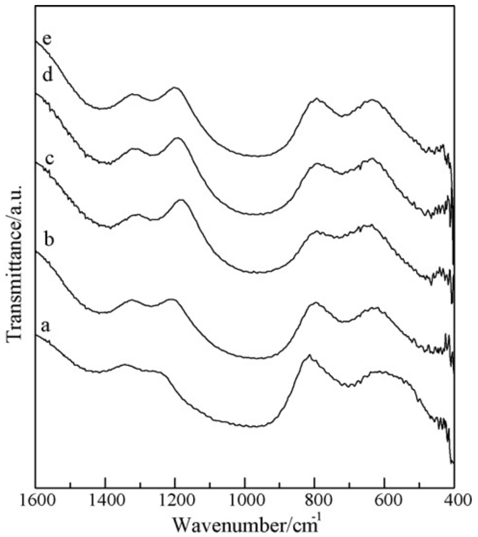

Fig. 1. IR spectra of glass powders: (a) glass 1# (b) glass 2# (c) glass 3# (d) glass 4# (e) glass 5#.

The DSC curves of the glasses are shown in Fig. 2. There is no exothermic peak for glass 1#, which indicates the glass being difficult to crystallize. In fact, the glass is only crystallized on the surface after reheating at 1100 °C. The glass transition temperature T_g is hardly changed for different samples at about 640 °C, but the crystallization temperature T_p decreases from 904 to 839 °C with MgO content increased from 13.4 to 31.4 mol%.

The $\Delta T = T_p - T_g$ is an important parameter to estimate the glass stability [23]. The bigger the ΔT is, the more stable the

Table 2
Observed IR absorption bands in studied glass system

Sample	Vibrations (cm^{-1})				
Glass 1#	1428	1294	979	707	451
Glass 2#	1422	1273	975	718	461
Glass 3#	1401	1267	969	723	467
Glass 4#	1401	1267	965	723	478
Glass 5#	1401	1267	959	726	472

Table 3
Vibration types of different IR wavenumbers

Frequency range (cm^{-1})	Type of vibration
<500	The bending vibration of O–Si–O and Si–O–Si [13]
600–850	The symmetric stretching vibration of Si–O–Si [13] and the stretching vibration of $[AlO_4]$ units [14]
~970	The asymmetric stretching vibration of Si–O–Si [15]
~1270	The asymmetric stretching vibration of $[BO_3]$ units [16,17]
1400	The bending vibration of O–H [18]

---

[1] Peralkaline compositions are those in which the number of moles of Al is less than the total charge due to monovalent and divalent cations, i.e., $[Al] < [M^+] < 2[M^{2+}]$.

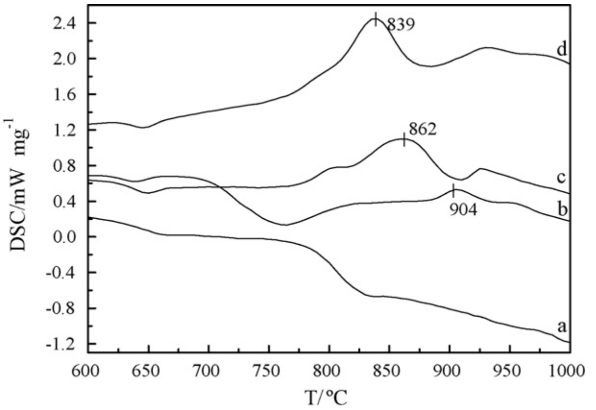

Fig. 2. DSC curves of glass samples subjected to the heating rate of 10 °C min^{-1}: (a) glass 1$^{\#}$, (b) glass 2$^{\#}$, (c) glass 3$^{\#}$ and (d) glass 5$^{\#}$.

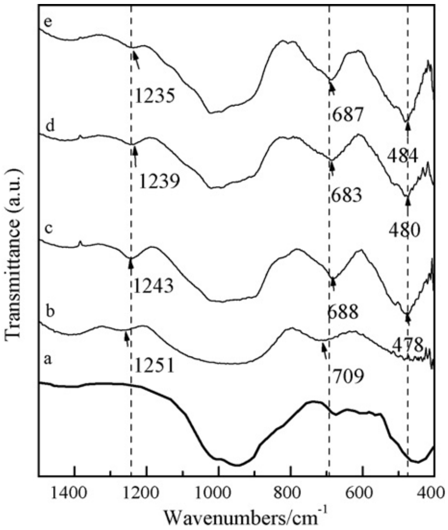

Fig. 4. IR spectra of: (a) phlogopite crystal, (b) glass 2$^{\#}$ and reheated at (c) 1000 °C, (d) 1050 °C, (e) 1100 °C.

glass will be. With the increase of MgO content, T_p is decreased, resulting in the decrease of ΔT from 264 to 200 °C, which suggests that the increase of MgO content may promote the formation of mica and improves the machinability of glass-ceramics.

XRD patterns of glass 2$^{\#}$ crystallized at 1000, 1050 and 1100 °C for 2 h are shown in Fig. 3. Flurophlogopite, aluminum magnesium spinel and fluo-pargrasite are observed in different glasses after reheated. With the increase of crystallization temperature, the contents of fluorophlogopite and aluminum magnesium spinel increase, while fluo-pargrasite decreases.

Fig. 4 shows the IR spectra of sample 2$^{\#}$ reheated at different temperatures. As a comparison, the IR spectrum of phlogopite crystal [24] is also pasted in Fig. 4. The IR spectra of all samples resemble that of phlogopite. With the increase of crystallization temperature, the strength of main absorption bands increases, which indicates the improvement of crystallinity of phlogopite. Mg^{2+} can induce the non-uniform arrangement of anionic charge [19]. With the increase of MgO content, the trend of phase separations increases gradually. Ca^{2+}, Mg^{2+} and K^{+} ions help to the balance of $[AlO_4]^-$ tetrahedron, contributing to the formation of $[AlO_4]_2Ca$, $[AlO_4]_2Mg$ and $[AlO_4]K$ complexes in glass networks. The excellent compatibility between the complexes and $[SiO_4]$ tetrahedron facilitates the formation of mica units $[AlSiO_3]$ [25]. Therefore, the short-range order existing in the glass structure is similar to the structure units of phlogopite, which is helpful for the formation of mica. When crystallization temperature is increased, the mobility of Mg^{2+} ions is increasing, resulting in crystal composition closer to stoichiometric phlogopite. It means higher reheating temperature to be helpful for the formation of mica.

Fig. 5 shows the XRD patterns of the glass-ceramics reheated at 1100 °C for 2 h. Flurophlogopite and spinel are precipitated at a magnesia content of 20.9 mol%. When the content of MgO is more than 24.5 mol% (the MgO stoichiometic in flurophlogopite), fluo-pargrasite, calcium fluorphlogopites and forsterite appear. Ca^{2+} ions are also bridged to each triple layers of mica, including flurophlogopite and calcium fluorpholopite. Spinel and forsterite crystals containing Mg^{2+} ions are also precipitated when the MgO content is over 24.5 mol%.

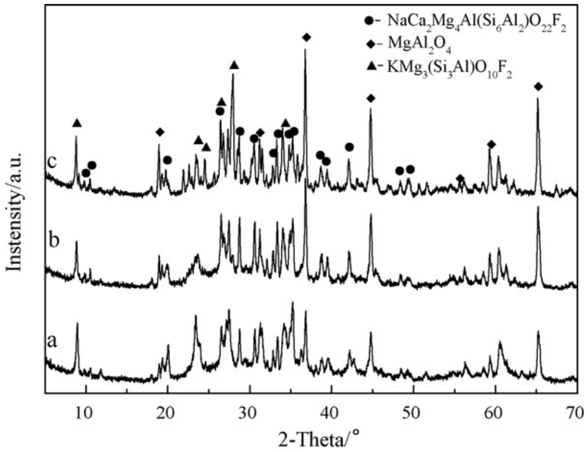

Fig. 3. XRD patterns of glass sample 2$^{\#}$ after different heat treatment: (a) 1000 °C 2 h, (b) 1050 °C, 2 h, (c) 1100 °C, 2 h.

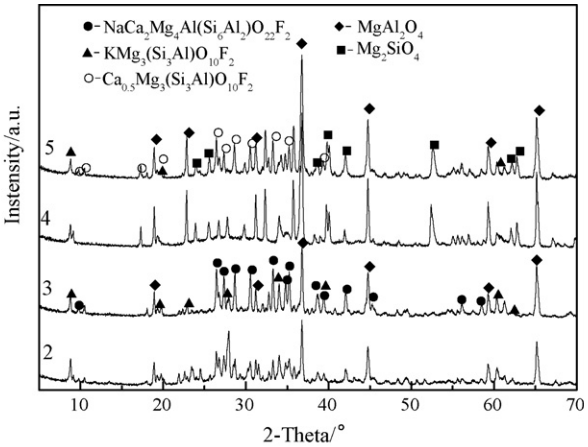

Fig. 5. XRD patterns of glass sample reheated at 1100 °C for 2 h.

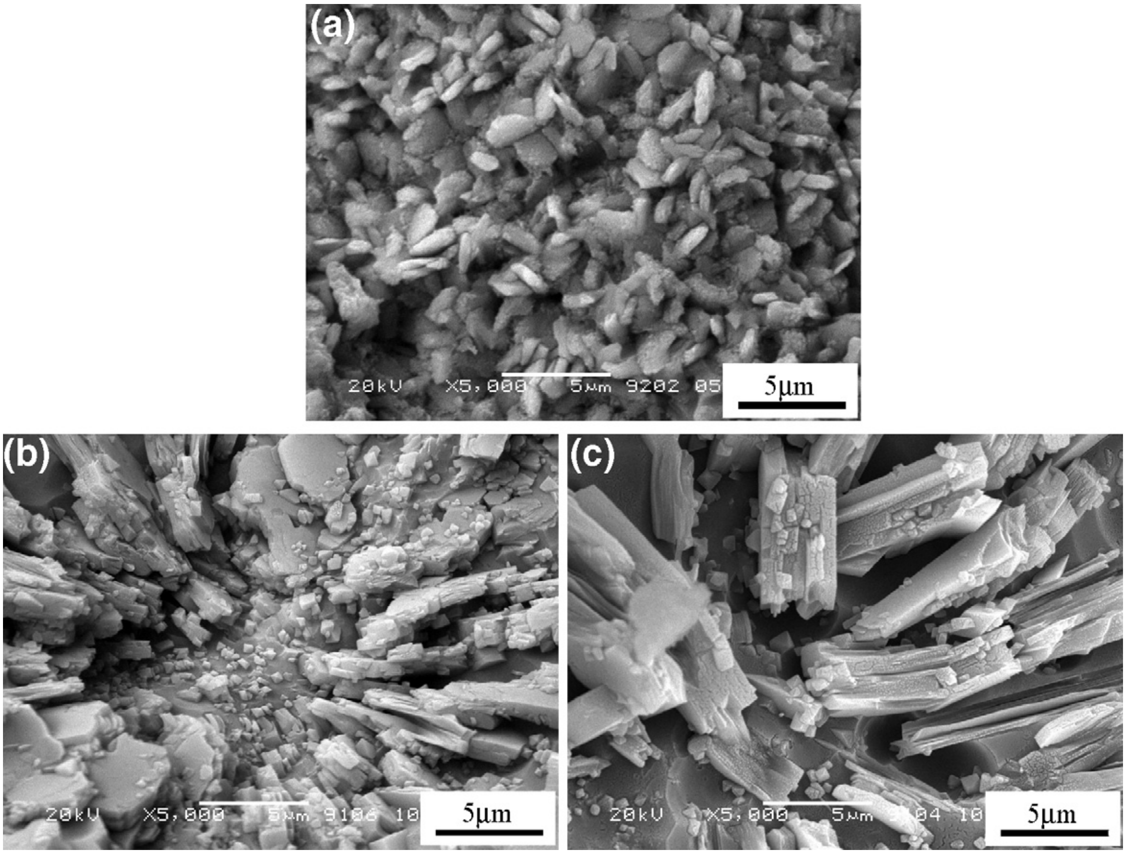

Fig. 6. SEM micrographs of glass-ceramics 2 reheated at: (a) 1000 °C, (b) 1050 °C and (c) 1100 °C.

Fig. 6 illustrates the development of microstructure of glass $2^{\#}$ crystallized at 1000, 1050 and 1100 °C for 2 h. The major crystal is layer mica. There are some octahedron crystals located among mica crystals, which should be aluminum magnesium spinel by EDX analysis. The result coincides with XRD analysis. Fig. 6c shows the crystals with a high aspect ratio (length/thickness).

The machinability of mica glass-ceramics is related to two main conditions: mica volume percent and degree of interlocking of crystalline phases [3]. The preferred aspect ratio of mica plate is beyond the two. The higher the aspect ratio, the lower the volume fraction of mica phase. It is required more than 30 vol.% of mica to attain machinability [26]. At high volume of mica percents, the crystal morphology becomes less important, since the degree of interlocking is already high. The aspect ratio of mica crystal increases with the increase of heat treatment temperature, resulting in an interconnected microstructure.

Micrographs of glass-ceramics with different MgO content reheated at 1100 °C are shown in Fig. 7. The degree of interlocking mica plates is increased with the increase of MgO content. Fig. 8 shows the plot of the aspect ratio of mica crystals

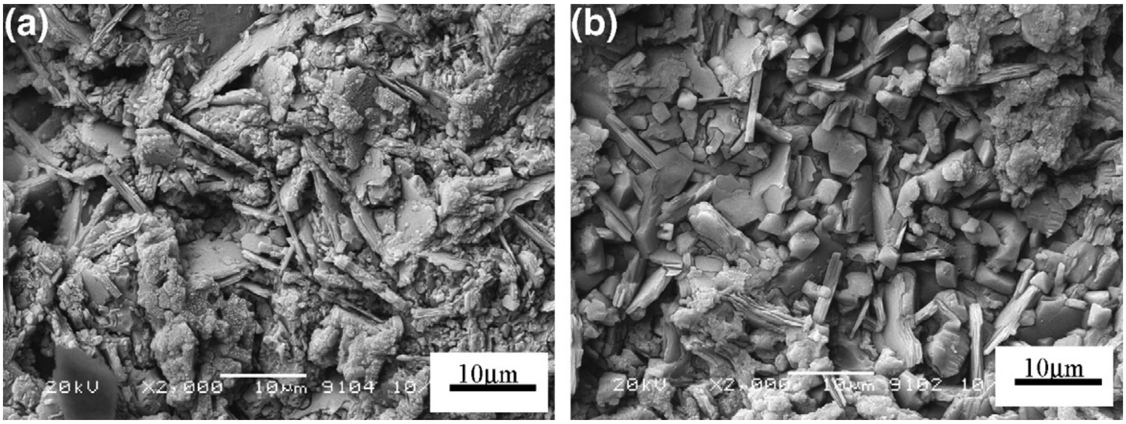

Fig. 7. SEM micrographs of glass $2^{\#}$ and $4^{\#}$ reheated at 1100 °C for 2 h.

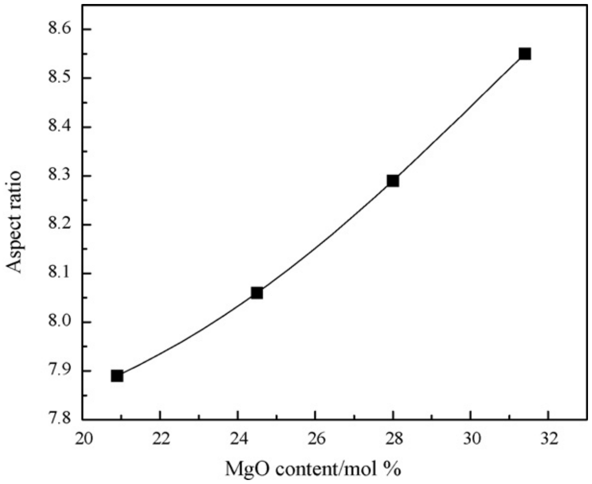

Fig. 8. Aspect ratio of phlogopite against MgO content after reheated at 1100 °C for 2 h.

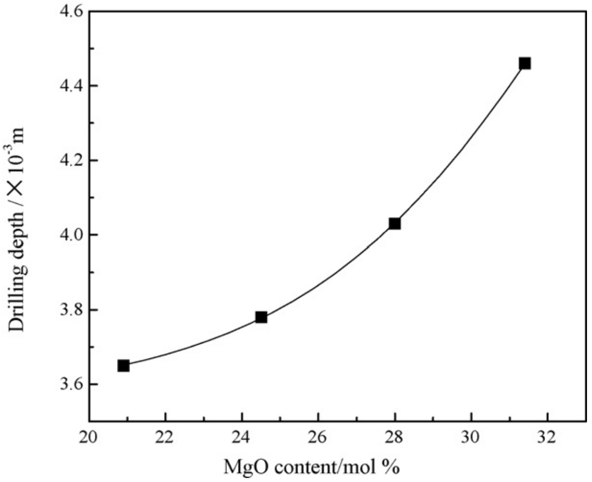

Fig. 9. Drilling depth of the glass-ceramics against MgO content after reheated at 1100 °C for 2 h.

versus the MgO content. The aspect ratio increases with the increase of MgO content and this is beneficial for the improvement of machinability. In Fig. 9, higher MgO content results in deeper drilling depth, indicating good machinability of mica glass-ceramics.

4. Conclusions

(1) The main units of glass network are [SiO_4] and [AlO_4] tetrahedra. The increase of MgO content contributes to the increase of NBOs, resulting in the decrease of the stability of the glass structure. [$AlSiO_3$] tetrahedron, similar to the structure unit of phlogopite, is considered to exit in the glasses.
(2) The addition of MgO increases the crystallization trend of the investigated glasses. Surface crystallization appears when MgO content is less than 13.4 mol%.
(3) The increase of crystallization temperature is helpful to the migration of Mg^{2+} ions, inducing the formation of phlogopite crystal. With the increase of phlogopite content and of its aspect ratio, the microstructure of the glass-ceramics becomes interconnected, which contributes to improve the machinability of the glass-ceramics.
(4) The higher the MgO content, the higher the aspect ratio. A higher aspect ratio is beneficial to machinability of glass-ceramics. Other phases containing magnesium (spinel, fluor-pargrasite, forsterite) are simultaneously precipitated when the content of MgO is over 24.5 mol%.

Acknowledgements

This work is supported by the National High Technology Research and Development Program of China (No. 2003AA332040) and the Scientific Research Fund of Hunan Normal University (No. 23040612).

References

[1] A.E. Mchale, Engineering properties of glass-ceramics, in: Engineered Materials Handbook, Ceramics and Glass, vol. 4, ASM International, Metals Park, OH, 1991, pp. 870–878.
[2] G.H. Beal, M.R. Montierth, G.P. Smith, Workable glass-ceramics, Tonind. Ztg. Keram 95 (12) (1971) 351–356.
[3] D.G. Grossman, Machinable glass-ceramics based on tetrasilicic mica, J. Am. Ceram. Soc. 55 (9) (1972) 446–449.
[4] K. Chyung, Fluorophlogopite mica glass-ceramics, in: Proceedings of 10th International Glass Congress, Ceramics Society of Japan, Tokyo, 1974, pp. 33–40.
[5] A. Gebhardt, T. Höche, G. Carl, et al., TEM study on the origin of cabbage-shaped mica crystal aggregates in machinable glass-ceramics, Acta Mater. 47 (17) (1999) 4427–4434.
[6] W. Vogel, W. Höland, Angew. Chem. 26 (1987) 527.
[7] K.G. Cheng, J.L. Wan, K.M. Liang, Enhance mechanical properties of oriented mica-ceramics, Mater. Lett. 39 (1999) 350–353.
[8] S. Habelitz, C. Rüssel, S. Thiel, et al., Mechanical properties of oriented mica glass ceramics, J. Non-Cryst. Solids 220 (1997) 291–298.
[9] S. Habelitz, G. Carl, C. Rüssel, Processing, microstructure and mechanical properties of extruded mica glass-ceramics, Mater. Sci. Eng. A 307 (2001) 1–14.
[10] J. Henry, R.G. Hill, The influence of Lithia content on the properties of fluorphlogopite glass-ceramics. I. Nucleation and crystallization behavior, J. Non-Cryst. Solids 319 (2003) 1–12.
[11] J. Henry, R.G. Hill, The influence of Lithia content on the properties of fluorphlogopite glass-ceramics. II. Microstructure hardness and machinability, J. Non-Cryst. Solids 319 (2003) 13–30.
[12] B. Eftekhari Yekta, S. Hashemi Nia, P. Alizadeh, The effect of B_2O_3, PbO and P_2O_5 on the sintering and machinability of fluormica glass-ceramics, J. Eur. Ceram. Soc. 25 (2005) 899–902.
[13] A.M. Efimov, Section 1. Optical properties of oxide glasses: quantitative IR spectroscopy: applications to studying glass structure and properties, J. Non-cryst. Solids 203 (1996) 1–11.
[14] C. Huang, E.C. Behrmsn, Structure and properties of calcium aluminosilicate glasses, J. Non-Cryst. Solids 128 (3) (1991) 210–321.
[15] A.M. Efimov, Vibrational spectra, related properties, and structure of inorganic glasses, J. Non-cryst. Solids 253 (1999) 95–118.
[16] E.I. Kamitsos, A.P. Patsis, et al., Infrared reflectance spectra of lithium borate glasses, J. Non-cryst. Solids 126 (1990) 52–67.
[17] A.K. Hassan, L. Borjesson, L.M. Torell, The boson peak in glass formers of in creasing fragility, J. Non-cryst. Solids 172/174 (1994) 154–160.
[18] M. Boczar, M.J. Wojcik, K. Szczeponek, Theoretical modeling of infrared spectra of aspirin and its deuterated derivative, Chem. Phys. 286 (2003) 63–79.

[19] C.I. Merzbcher, W.B. White, The structure of alkaline earth aluminosilicate glasses as determined by vibrational spectroscopy, J. Non-Cryst. Solids 130 (1) (1991) 18–34.

[20] C. Huang, E.C. Behrman, Structure and properties of calcium aluminosilicate glasses, J. Non-Cryst. Solids 128 (3) (1991) 310–321.

[21] S. Musić, J. Živko-Babić, K. Mehulić, et al., Microstructure of lucite glass-ceramics for dental use, Mater. Lett. 27 (4–5) (1996) 195–199.

[22] L. Stoch, M. Środa, Infrared spectroscopy in the investigation of oxide glasses structure, J. Mol. Struct. 511/512 (1999) 77–84.

[23] C.A. Angell, in: Proceedings of the Second International Symposium on Halide Glasses, Rensselaer Polytechnic Institute, Troy, NY, 1983, paper no. 8.

[24] W. Vedder, Correlations betweens infrared spectrum and chemical composition of mica, Am. Miner. 49 (5–6) (1964) 736–768.

[25] O.V. Mazurine, Phase Separation in Glass, North-Holland, Amsterdam, 1976, p. 125.

[26] B. Dmitri, P. Carlino, P. Paul, Machinable glass-ceramics, US Patent 066933, 4 February (2002).